

# Adaptive Gradient Prediction for DNN Training

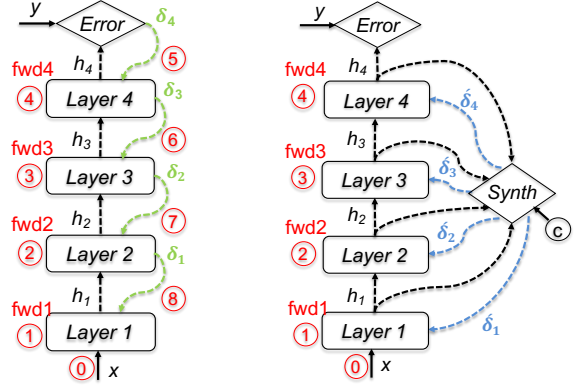
Vahid Janfaza, Shantanu Mandal, Farabi Mahmud, Abdullah Muzahid  
Department of Computer Science and Engineering, Texas A&M University, College Station, TX, USA  
{vahidjanfaza, shanto, farabi, abdullah.muzahid}@tamu.edu

## ABSTRACT

Neural network training is inherently sequential where the layers finish the forward propagation in succession, followed by the calculation and back-propagation of gradients (based on a loss function) starting from the last layer. The sequential computations significantly slow down neural network training, especially the deeper ones. Prediction has been successfully used in many areas of computer architecture to speed up sequential processing. Therefore, we propose ADA-GP, that uses gradient prediction adaptively to speed up deep neural network (DNN) training while maintaining accuracy. ADA-GP works by incorporating a small neural network to predict gradients for different layers of a DNN model. ADA-GP uses a novel tensor reorganization to make it feasible to predict a large number of gradients. ADA-GP alternates between DNN training using backpropagated gradients and DNN training using predicted gradients. ADA-GP adaptively adjusts when and for how long gradient prediction is used to strike a balance between accuracy and performance. Last but not least, we provide a detailed hardware extension in a typical DNN accelerator to realize the speed up potential from gradient prediction. Our extensive experiments with fourteen DNN models show that ADA-GP can achieve an average speed up of  $1.47\times$  with similar or even higher accuracy than the baseline models. Moreover, it consumes, on average, 34% less energy due to reduced off-chip memory accesses compared to the baseline hardware accelerator.

## 1. INTRODUCTION

Deep neural networks (DNNs) have shown remarkable success in recent years. They can solve various complex tasks such as recognizing images [27], translating languages [3, 48], driving cars autonomously [15], generating images/texts [39], playing games [42], etc. DNNs achieve their incredible problem solving ability by training on a vast amount of input data. The de facto standard for DNN training is the backpropagation algorithm [29]. The algorithm works by processing input data using the forward pass through the DNN model starting from the first layer to the last. The last layer computes a pre-defined loss function. Then, gradients are calculated based on the loss function and propagated back from the last layer to the first updating each layer's weights. Thus, the backpropagation algorithm is inherently sequential. A layer's weights cannot be updated until all the layers finish the forward pass and gradients are propagated back to that layer. This is shown in Figure 1a for an example 4-layer model where the gradients  $\delta_1, \dots, \delta_4$  are used for updating the



(a) Baseline DNN training.

(b) Training with gradient prediction.

Figure 1: DNN training baseline vs with gradient prediction.

weights.

The sequential nature of backpropagation algorithm makes DNN training a time consuming task. For decades, computer architects have been using *prediction* to speed up various processing tasks including sequential ones. For example, predicting branches, memory dependencies, memory access patterns, synchronizations, etc. have been used in various processor architectures to improve performance. Inspired by this line of research, we set out to investigate whether it is possible to use *gradient prediction* to relax the sequential constraints of DNN training.

There are two major challenges in gradient prediction.

1. *The Curse of Scale*: Scalability of gradient prediction arises from two aspects of a DNN model. *First*, the number of layers of any recent DNN model can be in the range of hundreds. Therefore, having one predictor for each layer is not scalable. *Second*, for many layers, the number of gradients (which should be equal to the number of weights of a layer) is quite large. In some cases, this number can exceed the number of output activations of a layer. Therefore, predicting a large number of gradients for a layer can be challenging.
2. *Accuracy vs. Performance*: Always using gradient prediction will speed up DNN training significantly (almost  $2x$  speed up by completely eliminating the backpropagation step) but can severely degrade the prediction accuracy. However, if a scheme focuses on predicting good quality gradients and uses them infrequently, it will not affect the prediction accuracy of the DNN model but reduce the speed up. Therefore, the scheme needs to adaptively decide when and how long to use gradient prediction during DNN training.

To address these challenges, we propose ADA-GP, the **first** scheme to use gradient prediction for speeding up DNN training while maintaining accuracy. ADA-GP works by incorporating a small neural network model, called *Predictor Model*, to predict gradients of various layers of a DNN model. ADA-GP uses a single predictor model for all layers. The model takes the output activations of a layer as inputs and predicts the gradients for that layer (as shown in Figure 1b). To predict a large number of gradients, ADA-GP uses tensor reorganization (details in Section 3.6) within a batch of input data. When training starts for a DNN model, the weights of the DNN model are initialized randomly. Therefore, the gradients for few training epochs (an epoch is defined as one iteration of DNN training using the entire dataset) are more or less random. So, ADA-GP uses the backpropagation algorithm as it is to train the DNN model for few (e.g., 10) initial epochs. During those epochs, ADA-GP trains the predictor model with the true gradients produced by the backpropagation algorithm. ADA-GP trains the predictor model with each layer’s gradients. After those initial epochs, ADA-GP alternates between DNN training using backpropagated gradients and DNN training using gradients predicted by the predictor model. In other words, for a number of batches (say,  $m$ ), ADA-GP trains the DNN model using the backpropagation algorithm as it is while training the predictor model with true gradients. We call this *Phase BP*. Then, for the next few batches (say,  $k$ ), ADA-GP switches to DNN training using predictor model generated gradients. We call this *Phase GP*. During Phase GP, the backpropagation algorithm is completely skipped leading to an accelerated training of the DNN model. Thus, ADA-GP alternates between Phase BP and Phase GP gradually adjusting the value of  $m$  and  $k$  to balance accuracy and performance. Finally, we propose some hardware extension in a typical DNN accelerator to implement ADA-GP and realize its full potential.

It should be noted that predicting gradients artificially (as opposed to using backpropagation algorithm) is not new. Several prior works investigate the possibility of utilizing synthetic gradients [1, 7, 8, 22, 32, 33, 35, 52]. This line of work is inspired by the biological learning process and produces synthetic gradients using some form of either controlled randomization or per-layer predictors. However, all of the techniques aim at producing better quality gradients for achieving prediction accuracy and convergence rate at least similar to that of backpropagation algorithm. *None of the existing techniques investigates synthetic gradients from performance improvement point of view.* Some techniques [32, 35] require forward propagation of all layers to finish before synthetic gradients can be produced. Majority of the techniques keeps the backpropagation computation as it is and requires similar or more training time compared to the backpropagation algorithm [7, 22, 33]. Some of the techniques introduce more trainable parameters into the model leading to an increased training time [2]. Last but not least, all of the existing techniques suffer from lower scalability, training stability and accuracy for deeper models.

## 1.1 Contributions

We make the following major contributions:

1. ADA-GP is the **first** work that has explored the idea of gradient prediction for improving DNN training time. It does so while maintaining the model accuracy.
2. ADA-GP uses a single predictor model to predict gradients for all layers of a DNN model. This reduces the storage and hardware overhead for gradient prediction. Moreover, ADA-GP uses a *novel* tensor reorganization technique among a batch of inputs to predict a large number of gradients.
3. ADA-GP uses backpropagated and predicted gradients alternatively to balance performance and accuracy. Moreover, ADA-GP adaptively adjusts when and for how long gradient prediction should be used. Thanks to this *novel* adaptive algorithm, ADA-GP is able to achieve both high accuracy and performance even for bigger DNN models with a larger dataset such as Imagenet.
4. We propose three possible extensions in a typical DNN accelerator with varying degree of resource requirements to realize the full potential of ADA-GP. Moreover, we show how ADA-GP can be utilized in a multi-chip environment with different parallelization techniques to further improve the performance gain.
5. We implemented ADA-GP in both FPGA and ASIC-style accelerators. We experimented with *fourteen* DNN models using three different dataset - CIFAR10, CIFAR100 and Imagenet. Our results indicate that ADA-GP can achieve an average speed up of  $1.47\times$  with similar or even higher accuracy than the baseline models. Moreover, due to the reduced off-chip memory accesses during the weight updates using predicted gradients, ADA-GP consumes 34% less energy compared to the baseline accelerator.

## 2. RELATED WORK

Jaderberg et al. [22] proposed Decoupled Neural Interface (DNI) where a layer receives synthetic gradients from an auxiliary model after output activations of the layer are calculated. The predicted gradients can be used to update the weights of the layer. The auxiliary model is trained based on the backpropagated gradients and the predicted gradients. In other words, DNI requires the backpropagation algorithm to proceed as usual. When a layer has the backpropagated gradients available, those gradients are compared against the predicted gradients, and the auxiliary model is updated. Thus, DNI does not eliminate the backpropagation step at all. Instead, it increases the computations of the backpropagation step by including the auxiliary model update as part of the backpropagation step. That is why, DNI does not improve training time. In fact, it slows down the training time. *This is different from ADA-GP, where the backpropagation step is adaptively skipped as the DNN training proceeds.* Speed up of ADA-GP comes from skipping the backpropagation step altogether. Moreover, the DNI approach was shown to work only for small networks (up to 6 layers) and small datasets such as MNIST. Czarnecki et al. [7] explored the benefits

of including derivatives in the learning process of the auxiliary model. The proposed method, called Sobolev Training (ST), considers both the second-order derivatives as well as the backpropagated gradients to train the auxiliary model. The intuition is that by including the derivatives, the auxiliary model will produce better-quality gradients compared to DNI. However, similar to DNI, it does not eliminate the backpropagation step. Rather, ST increases the backpropagation computation even more by including the computations of the second-order derivatives. Therefore, ST slows down the DNN training. Miyato et al. [33] proposed a virtual forward-backward network (VFBN) to simulate the actual sub-network above a DNN layer to generate gradients with respect to the weights of that layer. Thus, VFBN does not eliminate backpropagation at all. Instead, it introduces the backpropagation of a different network, namely VFBN. Using this approach, the authors showed comparative accuracy similar to the baseline model with backpropagation algorithm-based learning. However, similar to prior approaches, VFBN does not reduce the DNN training time.

There is a number of work that uses some form of random or direct gradients from the last layer. Promoting biological plausibility serves as a key motivation for the development of these techniques [1, 32, 35, 52], which target the removal of weight symmetry and potential gradient propagation in the backpropagation process. By substituting symmetrical weights with random ones, Feedback Alignment (FA) [32] achieves weight symmetry elimination. In continuation of FA [32], Direct FA [35] replaces the Backpropagation (BP) method with a random projection, possibly enabling concurrent updates for all layers. The study by Balduzzi et al. [1] disrupts local dependencies across consecutive layers, allowing direct error information reception by all hidden layers from the output layer. However, these approaches end up using poor-quality gradients. Therefore, they degrade the prediction accuracy of the DNN model significantly (especially for deeper models with a larger dataset) and eventually, end up taking more time to reach the target accuracy level. Decoupled Greedy Learning (DGL) [2], Decoupled Parallel Backpropagation (DDG) [21], and Fully Decoupled Training scheme (FDG) [54] are other strategies that aim to address sequential dependence problems of DNN training. While DDG and FDG have been shown to reduce total computation time, they incur large memory overhead due to the storage of a large number of intermediate results. Moreover, they also suffer from weight staleness. Following the DDG approach, Feature Replay (FR) [20] similarly breaks backward locking by recomputation and its performance has been shown to surpass BP in various deep architectures. However, FR has a greater computational demand, leading to a slower execution compared to DDG. Finally, these works require all layers to finish the forward propagation first before the weights can be updated. This is different from ADA-GP where weights of a layer can be updated as soon as the output activations are calculated. ADA-GP does not need to wait for the forward propagation of all layers to finish.

There are a number of parallelization strategies for DNN training. Data Parallelism [14, 30, 41, 53] is a widespread method for scaling up training processes on parallel machines, where each worker maintains a model copy and the

mini-batch is distributed among them. However, this method encounters efficiency challenges due to gradient synchronization or model size. Operator Parallelism offers a solution for training large models by dividing layer operators among workers but faces high communication volume. Hybrid techniques [24, 25] combining operator and data parallelism also encounter similar issues. Pipeline Parallelism [12, 19, 23, 31] has been extensively explored to reduce communication volume by partitioning the model layer-wise, assigning workers to pipeline stages, and processing micro-batches sequentially, thus improving resource utilization. However, ADA-GP is orthogonal to this line of work and can be applied in conjunction with any of these approaches.

### 3. ADAPTIVE GRADIENT PREDICTION

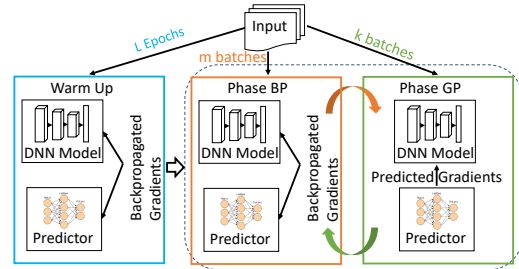


Figure 2: Overview of how ADA-GP uses gradient prediction for DNN training.

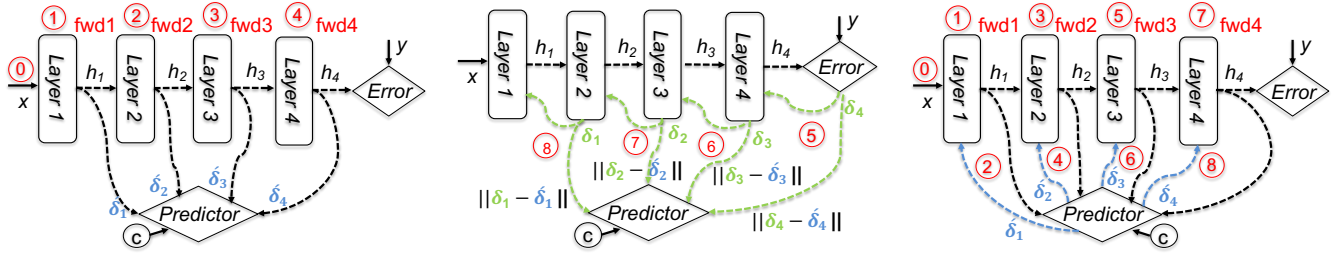
#### 3.1 Overview

ADA-GP works in three phases. When DNN training starts, the DNN model is initialized and trained using the backpropagation algorithm as it is. During the first few epochs (e.g.,  $L$  epochs), the predictor model is trained with the true (backpropagated) gradients without using any of the predicted gradients in model training. This is the *Warm Up* phase (this is reminiscent of warm up step used in the micro-architectural study). Keep in mind that an epoch is one iteration of DNN training with the entire input dataset. After that, ADA-GP alternates between backpropagation (Phase BP) and gradient prediction (Phase GP) phases within an epoch. In Phase BP, the DNN model as well as the predictor model is trained with backpropagated gradients. This is similar to the Warm Up phase except it lasts for few (say,  $m$ ) batches of input data during an epoch. Then, ADA-GP starts using the predicted gradients from the predictor model while skipping the backpropagation step altogether. The skipping of backpropagation leads an accelerated training in Phase GP. Phase GP lasts for few (say,  $k$ ) batches of input. After that, ADA-GP operates in Phase BP followed by Phase GP mode. This continues with the value of  $m$  and  $k$  adapting over time as the DNN training progresses. Thus, ADA-GP alternates between learning the actual gradients (from backpropagation) and applying the predicted gradients (after learning).

#### 3.2 Warm Up of ADA-GP

The intuition behind Warm Up phase is to initialize the predictor model and ramp up its gradient prediction ability.





(a) Forward propagation of ADA-GP in Phase BP.

(b) Backpropagation of ADA-GP in Phase BP.

(c) Overall training of ADA-GP in Phase GP.

Figure 3: The structure of ADA-GP in a) forward propagation of Phase BP, b) backward propagation of Phase BP, and c) comprehensive processes within Phase GP that train the initial model using the predicted gradients by predictor model.

Since the DNN model is initialized randomly, the backpropagated gradients are more or less random for the initial few epochs. The predictor model learns from those backpropagated gradients of each layer. As a result, the predicted gradients are even worse in quality during these epochs. That is why, ADA-GP does not apply the predicted gradients to update the DNN model. Instead, the backpropagated gradients are used for that purpose. Presumably, after few epochs, say  $L$ , the predictor starts to produce gradients that are close to the actual backpropagated gradients. Therefore, ADA-GP enters into Phase BP and GP.

### 3.3 Phase BP of ADA-GP

In Phase BP, both the original and predictor models are trained based on true gradients. Contrary to the DNI [22] method, which utilizes synthetic gradients for training the original model and true gradients for training the predictor model, Phase BP of ADA-GP calculates predicted gradients but does not apply them to the original model’s training. Instead, true gradients are employed for training both the original and predictor models. This technique maintains high accuracy for both models while retaining the performance as the DNI approach [22]. Figure 3a & 3b depict the training approach of Phase BP for an example of 4-layers DNN.

As illustrated in Figure 3a, unlike the DNI method, the weights of the layers are not updated during the forward propagation (steps ①, ②, ③, and ④) using predicted gradients. Nevertheless, the predicted gradients  $\delta'_1$ ,  $\delta'_2$ ,  $\delta'_3$ , and  $\delta'_4$  are still calculated with the predictor model based on the output activations in each layer. These predicted gradients are compared against the true gradients (i.e.,  $\delta_1$ ,  $\delta_2$ ,  $\delta_3$ , and  $\delta_4$ ) and the predictor model trained during the backward propagation. Figure 3b shows the backpropagation in Phase BP. As shown in Figure 3b, two operations are executed when calculating true gradients in each layer (steps ⑤, ⑥, ⑦, and ⑧): 1) the layer weights are updated, and 2) the predictor model is trained. As shown in these figures, in Phase BP, the original model undergoes the standard backpropagation step, while the predictor model is trained concurrently.

### 3.4 Phase GP of ADA-GP

In Phase GP, the standard backpropagation process is bypassed, and the original model is trained based on predicted gradients. Furthermore, the predictor model’s training is skipped in this phase. Figure 3c presents the ADA-GP pro-

cess in Phase GP. It is important to note that Phase GP is executed on a new input batch, following the completion of the previous batch’s process in Phase BP. As shown in Figure 3c, Phase GP does not have true gradients calculation, and it uses predicted gradients to update the original model’s weights. Also, in this phase, ADA-GP does not train the predictor model.

### 3.5 Adaptivity in ADA-GP

Following the Warm Up phase, ADA-GP transitions to the standard operation and adaptively alternates between the two primary phases - Phase BP and GP. Initially, it proceeds with Phase GP, utilizing the predicted gradients to train the original model. This phase persists for  $k$  batches before switching to Phase BP for  $m$  batches. At the outset,  $m < k$ . That means, at the beginning, ADA-GP uses predicted gradients more than the true gradients. ADA-GP gradually increases the value of  $m$  throughout the training process. As training gets closer to the end, the value of  $m$  becomes equal to  $k$ . From this point onward, the number of training batches in Phase BP equals to that in Phase GP until the end of the training, and ADA-GP no longer modifies  $m$ . The reasoning behind this approach is that the model is mostly random at the beginning and has a certain threshold regarding gradient accuracy. However, during the later epochs, the gradients’ changes need to be increasingly precise, necessitating higher quality gradients.

### 3.6 Tensor Reorganization

Often times, the predictor may need to predict a large number of gradients. For that purpose, ADA-GP rearranges the output activations of a DNN layer prior to forwarding them to the predictor model. This is done to 1) maintain the predictor model’s compact size, and 2) ensure high accuracy in the predicted gradients. As previously noted, we employ the output activations from each layer to predict the gradients for that specific layer.

The primary challenge in predicting the gradients of weights for each layer lies in the fact that the weight size in some layers is massive. When a small predictor tries to predict a large number of gradients, it not only produces poor-quality gradients but also increases the training time of the predictor itself. For example, consider layer 4 of the VGG13 model - Conv2d(in\_channels=128, out\_channels=256, kernel\_size=(3,3), stride=1, padding=1). In this layer, the output

activation size is (batch\_size, 256, 28, 28). Consequently, the number of trainable weight-related parameters that the predictor model should predict is  $128 \times 256 \times 3 \times 3$ . A simple predictor model with a single fully connected layer would require an input size of  $256 \times 28 \times 28$  and an output size of  $128 \times 256 \times 3 \times 3$ , necessitating substantial memory storage and increasing computational demands.

To address this issue, we introduce a *novel* tensor reorganization technique. First, we calculate the average along  $\text{dim}=0$  of the predictor model's input to account for the effects of all samples in a batch, resulting in an input tensor with  $\text{shape}=(256, 28, 28)$ . Recognizing that each layer's filters have unique impacts on output gradients, we can consider 256 as the batch size for the input. In our example, we have 256 filters with a size of  $128 \times 3 \times 3$ , generating an output with a channel size of 256 where each filter is individually convoluted with inputs to create a single output. With this explanation, the reshaped input to our predictor model becomes ( $\text{new\_batch\_size}=256, 1, 28, 28$ ), and the output shape should be ( $\text{new\_batch\_size}=256, 128 \times 3 \times 3$ ), which is relatively small for deep learning models. To generalize the predictor model for all layers in a large deep learning model, we utilize several pooling layers and a small Conv2d layer based on the input size, followed by a single fully connected layer responsible for predicting gradients. It is also essential to note that the fully connected layer size depends on the largest layer. Therefore, for smaller layers, we mask and skip output operations based on the required output size. Figure 4 shows the overall tensor reorganization step of ADA-GP for layer 4 of the VGG13 model.

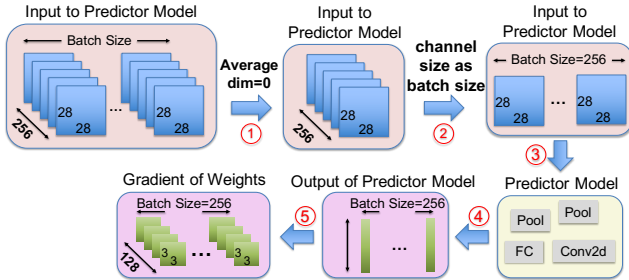


Figure 4: The overall architecture of the ADA-GP procedure for Layer 4 of VGG13: Conv2d(in\_channels=128, out\_channels=256, kernel\_size=(3,3), stride=1, padding=1). The predicted gradient dimensions should match the weight dimensions (128, 256, 3, 3). predictor model input (output activations) has the shape (batch\_size, 256, 28, 28).

### 3.7 Timeline of ADA-GP

Figure 5 illustrates the timeline of the baseline system for a 4-layer neural network model. We assume that the duration of the backward (BW) pass is twice as long as the forward (FW) pass. To simplify the explanation, we focus on the timeline for a single-chip system, although we will explore further details about multi-chip pipelining techniques in Section 3.8. As depicted in Figure 5, it is evident that the baseline system requires 12 time steps to complete the operation of a 4-layer model for a single batch. In this figure, the duration of each time step is equivalent to the FW time for

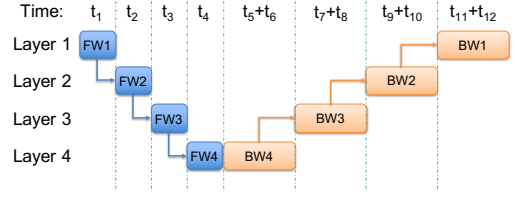


Figure 5: Baseline system timeline for a 4-layer DNN.

one layer. Throughout the remainder of this section, we will employ this definition of a *step* in our explanations. Figure 6 shows the timeline of ADA-GP in Phase BP. As mentioned in Section 3.3, during this phase, ADA-GP trains both the original and predictor models using true gradients in the BW pass. As illustrated in Figure 6, the delay of the FW process

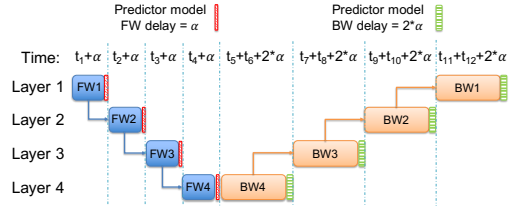


Figure 6: ADA-GP timeline in Phase BP.

in the predictor model can be observed, represented by  $\alpha$ . This delay is smaller than the FW pass duration in each layer of the original model. Consequently, the delay of the BW pass in the predictor model is set to  $2\alpha$ . As demonstrated in this figure, ADA-GP increases the model's training time by  $12\alpha$ . This value is directly linked to the predictor model's size and the number of operations in each FW and BW pass.

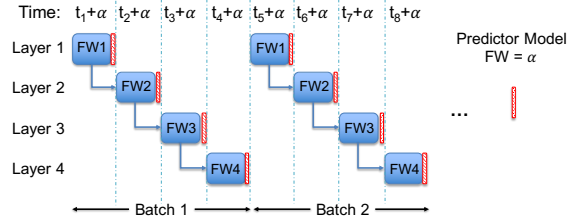


Figure 7: ADA-GP timeline in Phase GP.

Figure 7 presents the timeline of ADA-GP in Phase GP. As mentioned in Section 3.4, the BW process is skipped in this phase, and the predictor model is not trained. However, the original DNN model is trained using the predicted gradients generated by the predictor model. In Figure 7, it is evident that the BW pass is entirely eliminated, leaving only the FW pass of the initial model and a minor delay for the FW pass in the predictor model. Consequently, ADA-GP can minimize the processing time to merely  $4+4\alpha$  steps. As illustrated in Figures 3a, 3b, and 3c, ADA-GP is capable of decreasing the processing time for two epochs from 24 steps in the baseline system to  $16+16\alpha$ .

As an added benefit of skipping the BW pass in Phase GP, ADA-GP reduces off-chip traffic. Since the weights are updated as the FW pass proceeds, ADA-GP does not need to load the weights and activations from off-chip memory as is traditionally done in the case of BW pass. This significantly reduces energy consumption. More details are presented in Section 6.6.2.

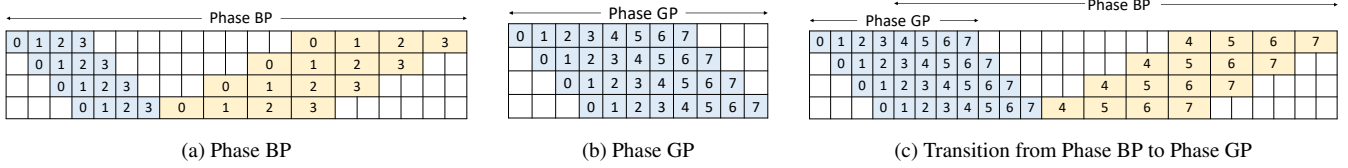


Figure 8: Structure of ADA-GP implemented over GPipe [19] a) Phase BP, b) Phase GP, and c) Phase BP to Phase GP.

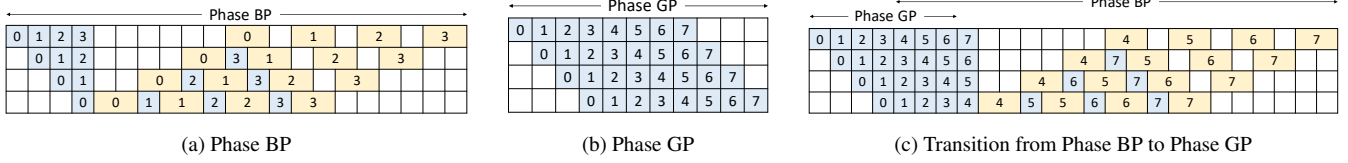


Figure 9: Structure of ADA-GP implemented over DAPPLE [12] a) Phase BP, b) Phase GP, and c) Phase BP to Phase GP.

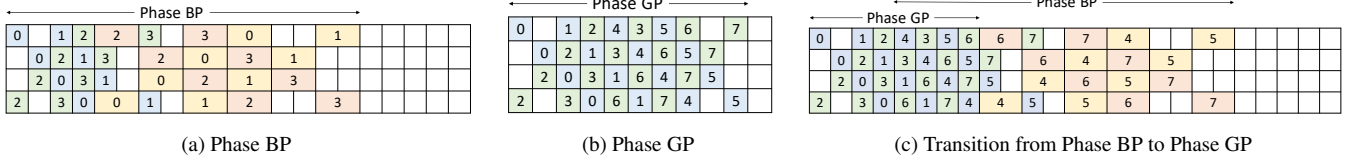


Figure 10: Structure of ADA-GP implemented over Chimera [31] a) Phase BP, b) Phase GP, and c) Phase BP to Phase GP.

### 3.8 ADA-GP in Multi-Device Hardware

Another approach to accelerating the training process involves utilizing multiple devices and employing some pipelining techniques to execute several layers concurrently. ADA-GP is orthogonal to this approach and can be integrated with it. To this end, we examine three prominent pipelining strategies - GPipe [19], DAPPLE [12], Chimera [31] and explain how ADA-GP can be incorporated with them to further speed up the training process. For ease of explanation, we assume in this section that there are four devices working concurrently, and the batch is divided into four segments, with each device processing one segment at a time.

Figure 8 shows how various ADA-GP phases work when implemented on top of the GPipe approach [19]. As depicted in Figure 8a, the ADA-GP operation in Phase BP is similar to the original GPipe method. Note that the duration of each step in ADA-GP differs from that in the original GPipe method. The step size of ADA-GP depends on its implementation as outlined in Section 4.2. Figure 8b shows the ADA-GP in Phase GP. In this figure, since ADA-GP eliminates the initial backpropagation process and employs predicted gradients for weight updates, it can initiate the subsequent batch’s process immediately after completing the current batch’s forward propagation. In doing so, ADA-GP can fill all gaps present in the original GPipe method. Lastly, Figure 8c illustrates how ADA-GP transitions from Phase BP to Phase GP without causing any additional delay. Another important point that should be taken into consideration is that ADA-GP reduces the number of synchronization steps to half and can save time and energy due to this reduction.

Figure 9 illustrates how various stages of ADA-GP can be integrated with the DAPPLE method [12]. Like the GPipe strategy, the configuration of ADA-GP in Phase BP closely resembles the original DAPPLE design. The depiction of ADA-GP during Phase GP can be observed in Figure 9b. As demonstrated in this figure, ADA-GP effectively eliminates the reliance between forward and backward propagation, fill-

ing all gaps in the training procedure. Additionally, Figure 9c portrays the shift from Phase BP to Phase GP.

The complete structure of the various stages of ADA-GP when implemented alongside the Chimera method [31] is depicted in Figure 10. As with earlier strategies, the structure of ADA-GP during Phase BP closely mirrors the initial Chimera design. In Phase GP, it is capable of operating all layers concurrently, eliminating any gaps. Furthermore, a transition between phases incurs no additional delays.

## 4. IMPLEMENTATION DETAILS

### 4.1 Baseline DNN Accelerator

Figure 11 illustrates a standard DNN accelerator design, featuring multiple hardware processing elements (PEs). These PEs are interconnected vertically and horizontally via on-chip networks. A global buffer stores input data, weights, and intermediate results. The accelerator is connected to external memory for inputs and outputs. Each PE is equipped with registers for holding inputs, weights, and partial sums, as well as multiplier and adder units. Inputs and weights are distributed across the PEs, which then generate partial sums following a specific dataflow.

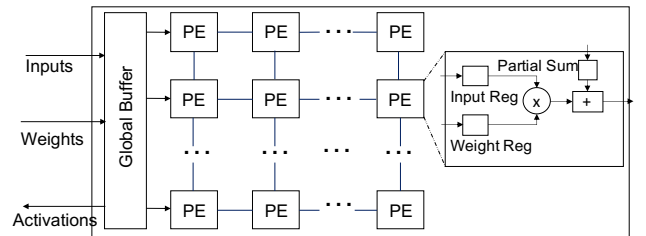


Figure 11: Baseline hardware accelerator.

Various dataflows have been suggested in the literature [5, 6, 28] to enhance different aspects of DNN operations, such

as Weight-Stationary (WS) [4, 13, 40], Output-Stationary (OS) [10], Input-Stationary (IS) [45], and Row-Stationary (RS) [5]. The dataflow’s designation often indicates which data remains constant in the PE during computation. In the Weight-Stationary (WS) approach, each PE retains a weight in its register, with operations utilizing the same weight assigned to the same PE unit [6]. Inputs are broadcasted to all PEs over time, and partial results are spatially reduced across the PE array after each time step. This method minimizes energy consumption by reusing filter weights and reducing weight reads from DRAM. Output-Stationary (OS) [38] focuses on accumulating partial results within each PE unit. At every time step, both input and filter weight are broadcasted across the PE array, with partial results calculated and stored locally in each PE’s registers. This method minimizes data movement costs by reusing partial results. Input-Stationary (IS) involves loading input data once and keeping it in the registers throughout the computation. Filter weights are unicast at each time step, while partial results are spatially reduced across the PE array. This strategy reduces the cost of sequentially reading input data from DRAM. Row-Stationary dataflow assigns each PE one row of input data to process. Filter weights stream horizontally, inputs stream diagonally, and partial sums are accumulated vertically. Row-Stationary has been proposed in Eyeriss [5] and is considered one of the most efficient dataflows to maximize data reuse.

## 4.2 ADA-GP Hardware Implementation

The general architecture of the ADA-GP is similar to the baseline accelerator shown in Figure 11. To implement ADA-GP, we propose three designs, striking a balance between hardware resource constraints and the degree of acceleration. Figure 12 shows the three distinct designs we proposed for ADA-GP. Figure 12a displays the architecture of ADA-GP-MAX. This configuration incorporates an additional PE Array and memory for predictor model computations and weights storage, respectively. Consequently, ADA-GP can initiate the predictor model’s gradient prediction operations concurrently with the original model’s computations, overlapping the processes and accelerating training. This design offers the most acceleration but also has more hardware overhead in comparison with other designs.

To offset the hardware overhead of ADA-GP-MAX, Figure 12b presents the ADA-GP-Efficient architecture. Instead of an extra PE array for the predictor model’s calculations, this design features a separate memory to store predictor model’s weights and commence its operations immediately after completing the original layer computations. While this configuration saves time and energy consumption related to reading and storing predictor’s weights, it must wait for the original model’s operation to finish before starting the predictor model computations.

Aiming to further reduce the hardware overhead of the ADA-GP design, Figure 12c depicts the ADA-GP-LOW structure. This layout eliminates all additional hardware overhead from the original design and reuses existing resources for predictor model computations. In essence, ADA-GP first completes the original model’s operations, then, after saving all necessary changes, loads the predictor’s weights and em-

loys the original PE Array for predictor model computations and updates. As demonstrated in Figure 12c, the overall architecture of ADA-GP-LOW closely resembles the baseline accelerator.

## 5. EXPERIMENTAL SETUP

### 5.1 ADA-GP Hardware Implementation

We implemented ADA-GP hardware in both FPGA and ASIC platforms. For FPGA implementation, we employed the Virtex 7 FPGA board [50], configured through the Xilinx Vivado [51] software. For ASIC implementation, the Synopsys Design Compiler [44] was used, and the design was developed using the Verilog language. Our implementation utilized a weight stationary accelerator with 180 PEs as the baseline. In the FPGA design, the model’s inputs and weights are stored in an external SSD connected to the FPGA. Block memories are employed to load one layer’s weights and inputs while storing the corresponding outputs. Performance, power consumption, hardware utilization, and other hardware-related metrics are gathered from the synthesized and placed and routed FPGA design using Vivado and the synthesized ASIC design using the Design Compiler.

### 5.2 ADA-GP Software Implementation

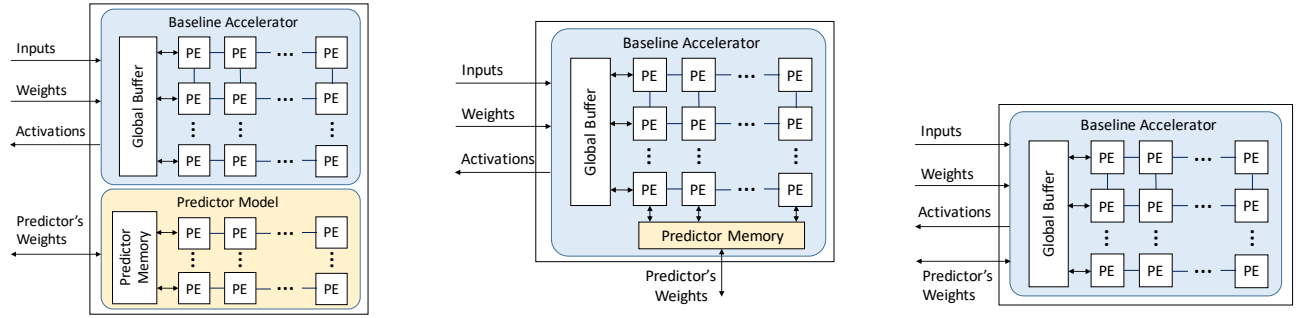
We gathered various model accuracy results from the PyTorch [37] implementation of ADA-GP. Fourteen networks are considered, including Inception-V4 [46], Inception-V3 [47], Densenet201 [18], Densenet169 [18], Densenet161 [18], Densenet121 [18], ResNet152 [16], ResNet101 [16], ResNet50 [16], VGG19 [43], VGG16 [43], VGG13 [43], MobileNet-V2 [17], and Transformer [49]. Our method is applied to three different datasets: ImageNet [9], Cifar100 [26], and Cifar10 [26]. For the transformer, we used the Multi30k [11] dataset and reported accuracy and BLEU scores [36] separately in Section 6.4.

During the training of ADA-GP and the baseline, the initial learning rate was set to 0.001 for the original models and 0.0001 for the predictor model. We employed SGD with Momentum and Adam optimizers for the original and predictor models, respectively. Additionally, we utilized the PyTorch ReduceLROnPlateau scheduler with default parameters for adaptive learning rate updates, while a MultiStepLR scheduler was applied for the predictor model scheduler. Top 1 accuracy was reported for the various models. To evaluate training costs, end-to-end training costs were calculated.

## 6. EVALUATION

Numerous previous studies have explored the potential of employing synthetic gradients in their research [1, 7, 8, 22, 32, 33, 35, 52]. These approaches generate synthetic gradients through controlled randomization or per-layer predictors. However, none of these methods focus on performance enhancement or skipping the backpropagation step. Moreover, their accuracy is less or equal to that of backpropagation-based training. Therefore, at best, those approaches will have





(a) ADA-GP-MAX architecture: This design employs distinct specialized PEs and memory for executing predictor model calculations. This allows for the simultaneous processing of predictor model operations alongside the original model.

(b) ADA-GP-Efficient architecture: This design does not have any specific PE-Array for predictor model computations however it has separate specific memory for saving the predictor's weights and can start the predictor model computations after finishing the original.

(c) ADA-GP-LOW architecture: This design has no specific hardware overhead for predictor model computations. Upon completion of the original model's operation, it initiates the predictor model's functioning by loading the predictor's weights.

Figure 12: Three distinct ADA-GP approaches, balancing the trade-off between hardware overhead and the degree of acceleration.

accuracy and performance similar to the backpropagation-based training. That is why, we use the backpropagation technique as our baseline to compare both the accuracy and performance of ADA-GP.

## 6.1 Accuracy Analysis

In this section, we evaluate the accuracy of the proposed method across thirteen different deep-learning models using three distinct datasets: ImageNet, Cifar100, and Cifar10, and compare it with the baseline Backpropagation (BP) approach.

	CIFAR10		CIFAR100		ImageNet	
	BP	ADA-GP	BP	ADA-GP	BP	ADA-GP
ResNet50	92.97	<b>93.76</b>	75.44	<b>75.73</b>	74.73	73.97
ResNet101	92.78	<b>93.62</b>	73.23	<b>75.38</b>	76.26	75.71
ResNet152	92.8	<b>93.12</b>	72.01	<b>73.7</b>	76.68	76.23
Inception-V4	91.22	<b>91.35</b>	70.52	<b>72.42</b>	76.23	75.9
Inception-V3	93.04	<b>93.88</b>	76.41	<b>77.68</b>	74.44	73.87
VGG13	91.52	<b>92.55</b>	70.48	70.41	70.68	<b>70.68</b>
VGG16	91.32	<b>92.34</b>	70.36	<b>70.47</b>	72.07	71.98
VGG19	91.18	<b>92.51</b>	69.69	<b>69.85</b>	72.94	72.83
DenseNet121	93.2	<b>93.63</b>	76.25	76.12	75.25	74.51
DenseNet161	93.48	<b>94.19</b>	76.87	<b>77.38</b>	76.43	<b>76.71</b>
DenseNet169	93.24	<b>94.15</b>	75.57	<b>76.4</b>	75.36	75.3
DenseNet201	93.26	<b>94.13</b>	76.37	<b>76.96</b>	75.52	<b>75.56</b>
MobileNet	90.08	<b>91.34</b>	68.11	<b>68.47</b>	69.88	69.23

Table 1: Accuracy comparison between ADA-GP and Baseline (BP) for CIFAR10, CIFAR100 & ImageNet dataset.

Table 1 presents the accuracy comparison between the proposed ADA-GP and baseline BP for the Cifar10, Cifar100, and ImageNet datasets. As shown in this table, in the Cifar10 dataset, ADA-GP effectively boosted the accuracy of all models by as much as 1.45% and an average of 0.75%. When applied to the Cifar100 dataset, ADA-GP similarly yielded improvements, with accuracy enhancements of up to 2.15% and an average gain of 0.88%. To further verify the efficacy of our approach, we applied ADA-GP on the ImageNet dataset. The final two columns of Table 1 reveal

that ADA-GP preserved the accuracy of all models at levels nearly equivalent to the baseline (BP), with a negligible average reduction of 0.3%. In certain cases, such as with DenseNet161 and DenseNet201 our proposed method even increased accuracy by 0.28% and 0.04% respectively, and in VGG13, the accuracy remained unchanged.

## 6.2 Case Study: VGG13

We perform an in-depth analysis of VGG13, decomposing the training costs across various layers by employing the ADA-GP-Efficient approach as well as the conventional BP technique. The outcomes can be seen in Figure 13. Regarding the ADA-GP-Efficient method, we divide the costs into three parts, each corresponding to distinct stages of the training process such as Warm-up (step 1 + step 2), Phase BP, and Phase GP.

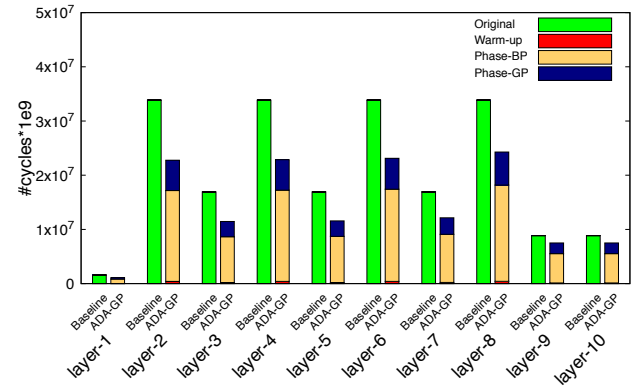


Figure 13: Characterization of ADA-GP in VGG13.

## 6.3 Performance Analysis

In the ADA-GP-MAX approach, during Phase BP, the forward pass (FW) of the predictor model can be computed simultaneously with the FW of the subsequent layer, as well as the backward pass (BW) of the predictor model alongside the BW of that layer. This method allows us to nearly eliminate the predictor model's operation in Phase GP, but we must still determine the maximum between the original and



predictor models. It is essential to wait for the current layer to complete its operation before proceeding to the next layer to avoid conflicts between the operations of different layers.

In the ADA-GP-Efficient method, the predictor’s weights are constantly stored in designated memory; however, there is no additional processing element (PE) to perform the predictor model’s operation in parallel with the original model’s operations. Consequently, the cost of each layer equals the sum of the original model and predictor model costs in distinct phases. Similar to the ADA-GP-MAX approach, the operations between layers are synchronized, initiating the subsequent layer’s operation only after the current layer’s operation is completed.

In the ADA-GP-LOW approach, there is no additional memory allocated for the predictor model weights, requiring us to load them after each original layer operation. Consequently, the expense associated with each layer should encompass the loading of predictor model weights and the storage of computed results. Nonetheless, following the loading process, the number of operations would be akin to the ADA-GP-Efficient approach. Given that we will only take this method into account for hardware overhead calculations and disregard its results in this section.

Figures 14a, 14b, and 14c display the overall acceleration of ADA-GP-Efficient and ADA-GP-MAX in comparison to the baseline system. In these figures, the baseline system represents a standard BP process utilizing the Weight-Stationary (WS) dataflow. The performance metrics are reported in relation to the dataset, as the model’s structure exhibits slight changes depending on the input size in different datasets. As demonstrated in these figures, ADA-GP-MAX can enhance the training process by up to  $1.51\times$ ,  $1.51\times$ , and  $1.58\times$  for the Cifar10, Cifar100, and ImageNet datasets, respectively. Furthermore, it expedites the process by an average of  $1.46\times$ ,  $1.46\times$ , and  $1.48\times$  across all models for the Cifar10, Cifar100, and ImageNet datasets, respectively.

We also perform analogous experiments for the Row Stationary (RS) dataflow. Figure 15 illustrates the overall acceleration of ADA-GP-Efficient and ADA-GP-MAX compared to the RS baseline. Figures 15a, 15b, and 15c indicate that ADA-GP-MAX can boost the training process by up to  $1.48\times$  for each of the Cifar10, Cifar100, and ImageNet datasets. Additionally, it increases the training speed on average by  $1.46\times$  across Cifar10 and Cifar100 datasets respectively, and  $1.47\times$  in the ImageNet dataset.

In a similar vein, we carried out additional experiments to demonstrate the acceleration of ADA-GP-Efficient and ADA-GP-MAX over the Input-Stationary (IS) dataflow baseline. Figure 16 presents a summary of these experimental results. Figures 16a, 16b, and 16c reveal that ADA-GP-MAX can enhance the training process by an average of  $1.46\times$ ,  $1.46\times$ , and  $1.48\times$  for the Cifar10, Cifar100, and ImageNet datasets, respectively.

## 6.4 Evaluation with Transformer Model

In this segment, we employed the ADA-GP technique on a Transformer model consisting of three encoding and decoding layers. We distinguish the Transformer model from other deep learning models due to the different datasets employed

for it.

To assess our approach, we utilized the Multi30k [11] English-German translation dataset. Table 2 shows the overall accuracy and performance comparison of ADA-GP with baseline (BP) design. As demonstrated in Table 2, ADA-GP

	Val Acc.	loss	BLEU Score	#Cycles( $\times 10^9$ )
Baseline(BP)	52.42	1.61	33.52	1245.87
<b>ADA-GP</b>	52.14	1.65	33.4	1104.31

Table 2: Accuracy and performance comparison between ADA-GP and Baseline (BP) for Multi30k dataset.

accelerates the training process of the Transformer by a factor of  $1.13\times$ . Furthermore, ADA-GP does not adversely impact the model’s performance and maintains the high accuracy of the Transformer model, achieving nearly identical BLEU Score [36] results.

## 6.5 Multi-Device Comparative Analysis

In this section, we evaluate the performance of the proposed ADA-GP relative to different baseline pipelining techniques using the ImageNet dataset in the context of multi-device hardware systems including GPipe [19], DAPPLE [12], and Chimera [31]. We employ the scenario outlined in section 3.8 to compute the training acceleration. We consider a setup with four devices operating concurrently, where each mini-batch is split into four portions (macro-batch), and each device processes one macro-batch at a time. Similarly, we can implement ADA-GP across diverse multi-device hardware systems with varying numbers of devices, offering additional savings on top of their existing configurations. In this section, the duration of each time step is equivalent to the delay of the FW process in a single device for one macro-batch. Throughout the remainder of this section, we will employ this definition of a *step* in our explanations.

### 6.5.1 Comparison with GPipe

As depicted in Figure 8, the standard GPipe method takes 21 steps to complete the training of *one* batch. ADA-GP can significantly reduce computations in Phase GP by eliminating the conventional backpropagation process. Also, when transitioning from Phase GP to Phase BP, ADA-GP only requires 25 steps to finish the training of *two* batches. Figure 17a depicts the overall acceleration of ADA-GP in comparison to the baseline GPipe method. As seen in Figure 17a, ADA-GP accelerates the training process for all deep learning models, achieving up to  $1.68\times$  speedup and an average of  $1.654\times$  improvement.

### 6.5.2 Comparison with DAPPLE

As illustrated in Figure 9, the DAPPLE method [12], similar to GPipe technique, requires 21 steps to complete the training of one batch. The timing of the ADA-GP when applied to DAPPLE also resembles that of the GPipe technique, taking into account the fact that the delay is associated with the DAPPLE design. Figure 17b demonstrates the extent of ADA-GP acceleration for various deep learning models com-

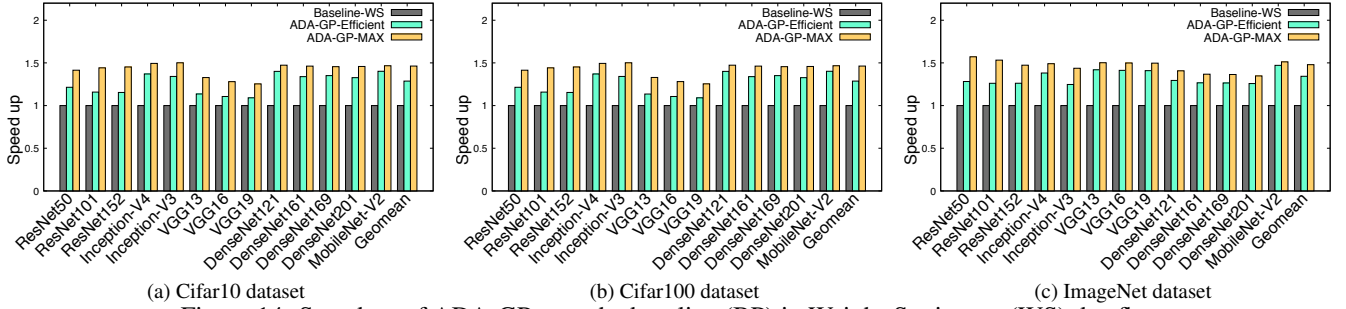


Figure 14: Speed up of ADA-GP over the baseline (BP) in Weight-Stationary (WS) dataflow.

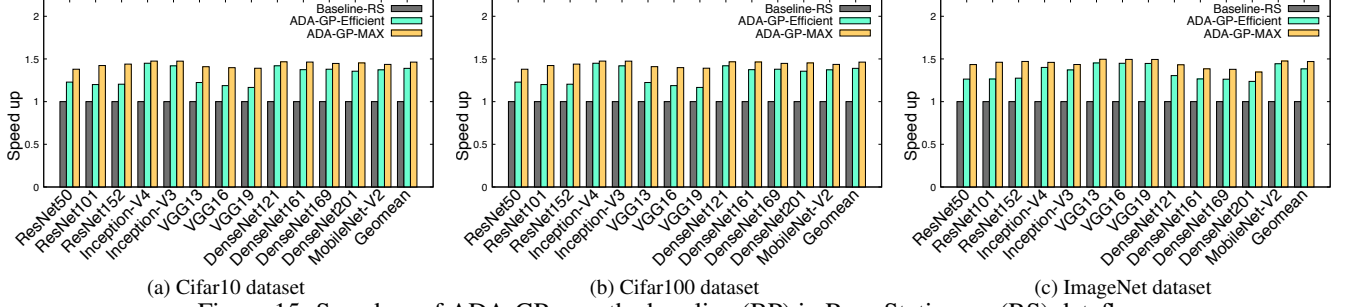


Figure 15: Speed up of ADA-GP over the baseline (BP) in Row-Stationary (RS) dataflow.

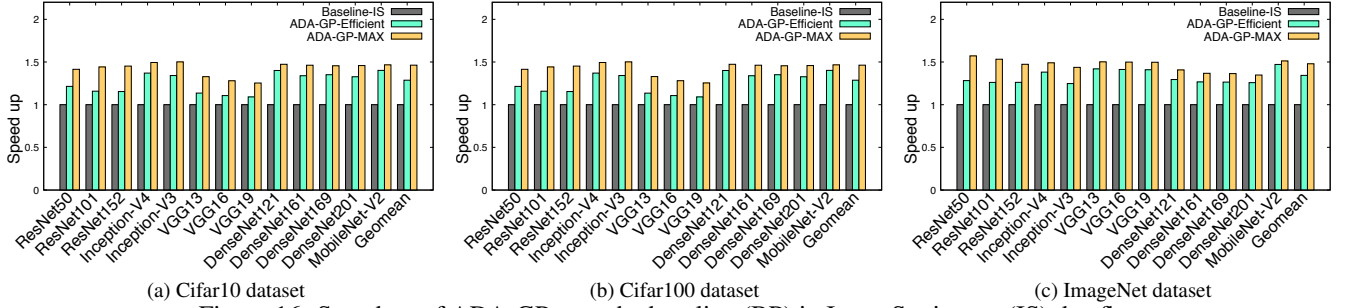


Figure 16: Speed up of ADA-GP over the baseline (BP) in Input-Stationary (IS) dataflow.

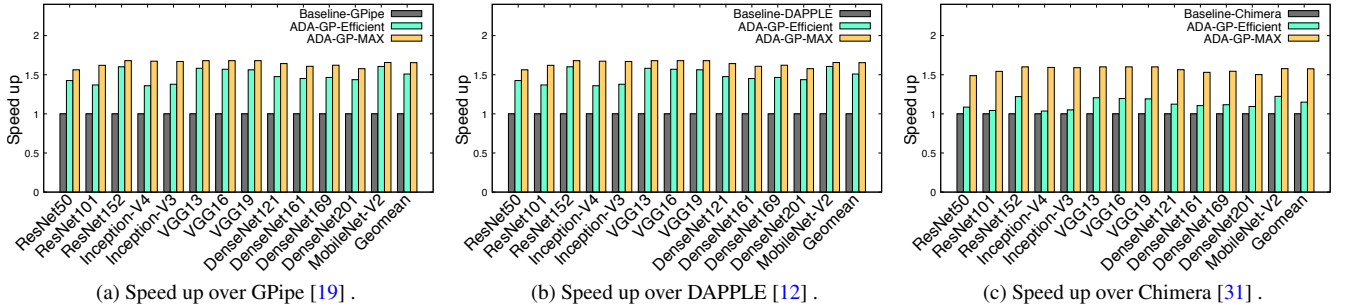


Figure 17: Speed up of ADA-GP over the baseline pipelining techniques a) GPipe [19], b) DAPPLE [12], and c) Chimera [31].

pared to the baseline DAPPLE design, achieving a maximum speedup of  $1.68\times$  and an average improvement of  $1.654\times$ .

### 6.5.3 Comparison with Chimera

The cutting-edge Chimera [31] technique surpasses all prior methods, potentially addressing numerous gaps in deep learning model training. The Chimera approach manages to complete *one* batch's training in just 16 steps. By incorporating the ADA-GP into the Chimera method, not only do we retain all previous savings during Phase GP, but also when transitioning from Phase GP to Phase BP, the scheme

necessitates merely 20 steps to finish training *two* batches. Figure 17c provides a detailed breakdown of the ADA-GP training acceleration for a range of deep learning models. As a result, the scheme effectively speeds up the Chimera training process for these models by up to  $1.6\times$  and, on average,  $1.575\times$ .

## 6.6 Hardware Analysis

In this section, we discuss the resource usage and power consumption of ADA-GP for both ASIC and FPGA implementations. Additionally, we provide a detailed comparison

of the energy consumption between ADA-GP and the baseline design. We employed CACTI [34] to incorporate cache and memory access time, cycle time, area, leakage, and dynamic power model to calculate the design’s energy consumption.

### 6.6.1 ADA-GP Hardware Implementation Analysis

As mentioned in section 4.2, we proposed three unique designs: ADA-GP-LOW, ADA-GP-Effective, and ADA-GP-MAX, with the goal of balancing acceleration levels and hardware resources. In Table 3, we examine the differences in resource usage and on-chip energy consumption between these ADA-GP designs and the baseline for the FPGA implementation.

	#CLB LUTs	#CLB Registers	#Block RAMB36	#Block RAMB18	#DSP48E1s
Baseline	472004	31402	1327	514	166
ADA-GP-LOW	489286	31856	1327	514	166
ADA-GP-Effic.	493171	31916	2407	514	166
ADA-GP-MAX	494080	37452	2407	514	246

(a) Resource Utilization

	Clocks	CLB Logic	Signals	Block RAM	DSPs	Static	Total
Baseline	0.046	0.42	0.842	0.244	0.009	2.032	3.712
ADA-GP-LOW	0.047	0.446	0.857	0.243	0.001	2.032	3.745
ADA-GP-Effic.	0.052	0.421	0.852	0.339	0.001	2.06	3.844
ADA-GP-MAX	0.055	0.426	0.857	0.339	0.001	2.059	3.856

(b) On-chip Power Consumption (watt)

Table 3: a) Resource usage and b) On-chip power consumption (watt) of different structures of ADA-GP vs baseline design in FPGA implementation.

As illustrated in Table 3, the ADA-GP-LOW, ADA-GP-Effective, and ADA-GP-MAX designs result in a power increase of only 0.8%, 3.5%, and 3.8%, respectively. This rise in power consumption is due to the additional hardware incorporated in the various designs.

Table 4 contrasts the area and energy consumption of the different ADA-GP designs with the baseline in the ASIC implementation.

	Combinational	Buf/Inv	Net Intercon.	Total Cell	Total Area
Baseline	2331250	272483	436615	2546076	2982691
ADA-GP-LOW	2375188	277261	445371	2590583	3035954
ADA-GP-Effic.	2405881	275783	440031	2622858	3062890
ADA-GP-MAX	2512057	287076	460157	2770979	3231136

(a) Area

	Internal	Switching	Leakage	Total
Baseline	2.26E+04	1.72E+03	1.99E+05	2.24E+05
ADA-GP-LOW	2.25E+04	1.67E+03	2.02E+05	2.26E+05
ADA-GP-Effic.	2.27E+04	1.80E+03	2.00E+05	2.25E+05
ADA-GP-MAX	2.80E+04	2.42E+03	2.23E+05	2.54E+05

(b) Power ( $\mu$  watt)

Table 4: a) Area and b) power consumption (watt) of different structures of ADA-GP vs baseline design in ASIC implementation.

As depicted in Table 4, the ADA-GP-LOW, ADA-GP-

Efficient, and ADA-GP-MAX designs lead to an increase in the final design area by 1.7%, 2.6%, and 8.3%, respectively. This also results in a rise in the design power.

### 6.6.2 Energy Consumption Analysis

In Figure 18, the energy consumption associated with memory access during the training process for both the baseline and ADA-GP methods is compared. As a result, ADA-GP enhances energy efficiency for all models, resulting in an average reduction of energy consumption by 34%.

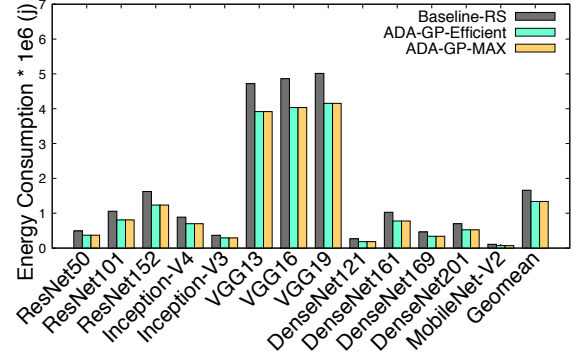


Figure 18: The energy consumption comparison between baseline back propagation and ADA-GP designs.

It is worth mentioning that the presented results do not take into account the savings achieved by reducing the number of synchronization steps, but only reflect the savings from reducing the number of memory read/write operations.

## 7. CONCLUSIONS

In this paper, we proposed ADA-GP, the **first** approach to use gradient prediction to improve the performance of DNN training while maintaining accuracy. ADA-GP warms up the predictor model during the initial few epochs. After that ADA-GP alternates between using backpropagated gradients and predicted gradients for updating weights. As the training proceeds, ADA-GP adaptively decides when and for how long gradient prediction should be used. ADA-GP uses a single predictor model for all layers and uses a *novel* tensor reorganization to predict a large number of gradients. We experimented with different DNN models using three different dataset - CIFAR10, CIFAER100 and Imagenet. Our results indicate that ADA-GP can achieve an average speed up of 1.47 $\times$  with similar or even higher accuracy than the baseline models. Moreover, due to the reduced off-chip memory accesses during the weight updates, ADA-GP consumes 34% less energy compared to the baseline accelerator.

## REFERENCES

- [1] D. Balduzzi, H. Vanchinathan, and J. Buhmann, “Kickback cuts backprop’s red-tape: Biologically plausible credit assignment in neural networks,” in *Proceedings of the AAAI Conference on Artificial Intelligence*, vol. 29, no. 1, 2015.
- [2] E. Belilovsky, M. Eickenberg, and E. Oyallon, “Decoupled greedy learning of cnns,” in *International Conference on Machine Learning*. PMLR, 2020, pp. 736–745.



- [3] T. B. Brown, B. Mann, N. Ryder, M. Subbiah, J. Kaplan, P. Dhariwal, A. Neelakantan, P. Shyam, G. Sastry, A. Askell, S. Agarwal, A. Herbert-Voss, G. Krueger, T. Henighan, R. Child, A. Ramesh, D. M. Ziegler, J. Wu, C. Winter, C. Hesse, M. Chen, E. Sigler, M. Litwin, S. Gray, B. Chess, J. Clark, C. Berner, S. McCandlish, A. Radford, I. Sutskever, and D. Amodei, "Language models are few-shot learners," 2020.
- [4] S. Chakradhar, M. Sankaradas, V. Jakkula, and S. Cadambi, "A dynamically configurable coprocessor for convolutional neural networks," in *Proceedings of the 37th annual international symposium on Computer architecture*, 2010, pp. 247–257.
- [5] Y. Chen, J. Emer, and V. Sze, "Eyeriss: A spatial architecture for energy-efficient dataflow for convolutional neural networks," in *2016 ACM/IEEE 43rd Annual International Symposium on Computer Architecture (ISCA)*, 2016, pp. 367–379.
- [6] Y. Chen, J. Emer, and V. Sze, "Using dataflow to optimize energy efficiency of deep neural network accelerators," *IEEE Micro*, vol. 37, no. 3, pp. 12–21, 2017.
- [7] W. M. Czarnecki, S. Osindero, M. Jaderberg, G. Swirszcz, and R. Pascanu, "Sobolev training for neural networks," *Advances in neural information processing systems*, vol. 30, 2017.
- [8] W. M. Czarnecki, G. Świrszcz, M. Jaderberg, S. Osindero, O. Vinyals, and K. Kavukcuoglu, "Understanding synthetic gradients and decoupled neural interfaces," in *International Conference on Machine Learning*. PMLR, 2017, pp. 904–912.
- [9] J. Deng, W. Dong, R. Socher, L.-J. Li, K. Li, and L. Fei-Fei, "ImageNet: A Large-Scale Hierarchical Image Database," in *CVPR09*, 2009.
- [10] Z. Du, R. Fasthuber, T. Chen, P. Ienne, L. Li, T. Luo, X. Feng, Y. Chen, and O. Temam, "Shidiannao: Shifting vision processing closer to the sensor," in *Proceedings of the 42nd Annual International Symposium on Computer Architecture*, 2015, pp. 92–104.
- [11] D. Elliott, S. Frank, K. Sima'an, and L. Specia, "Multi30K: Multilingual English-German image descriptions," in *Proceedings of the 5th Workshop on Vision and Language*. Berlin, Germany: Association for Computational Linguistics, Aug. 2016, pp. 70–74. [Online]. Available: <https://aclanthology.org/W16-3210>
- [12] S. Fan, Y. Rong, C. Meng, Z. Cao, S. Wang, Z. Zheng, C. Wu, G. Long, J. Yang, L. Xia *et al.*, "Dapple: A pipelined data parallel approach for training large models," in *Proceedings of the 26th ACM SIGPLAN Symposium on Principles and Practice of Parallel Programming*, 2021, pp. 431–445.
- [13] V. Gokhale, J. Jin, A. Dundar, B. Martini, and E. Culurciello, "A 240 g-ops/s mobile coprocessor for deep neural networks," in *Proceedings of the IEEE conference on computer vision and pattern recognition workshops*, 2014, pp. 682–687.
- [14] P. Goyal, P. Dollár, R. Girshick, P. Noordhuis, L. Wesolowski, A. Kyrola, A. Tulloch, Y. Jia, and K. He, "Accurate, large minibatch sgd: Training imagenet in 1 hour," *arXiv preprint arXiv:1706.02677*, 2017.
- [15] S. Grigorescu, B. Trasnea, T. Cocias, and G. Macesanu, "A survey of deep learning techniques for autonomous driving," *Journal of Field Robotics*, vol. 37, no. 3, pp. 362–386, apr 2020. [Online]. Available: <https://doi.org/10.1002%2Frob.21918>
- [16] K. He, X. Zhang, S. Ren, and J. Sun, "Deep residual learning for image recognition," in *Proceedings of the IEEE conference on computer vision and pattern recognition*, 2016, pp. 770–778.
- [17] A. Howard, A. Zhmoginov, L.-C. Chen, M. Sandler, and M. Zhu, "Inverted residuals and linear bottlenecks: Mobile networks for classification, detection and segmentation," 2018.
- [18] G. Huang, Z. Liu, L. Van Der Maaten, and K. Q. Weinberger, "Densely connected convolutional networks," in *Proceedings of the IEEE conference on computer vision and pattern recognition*, 2017, pp. 4700–4708.
- [19] Y. Huang, Y. Cheng, A. Bapna, O. Firat, D. Chen, M. Chen, H. Lee, J. Ngiam, Q. V. Le, Y. Wu *et al.*, "Gpipe: Efficient training of giant neural networks using pipeline parallelism," *Advances in neural information processing systems*, vol. 32, 2019.
- [20] Z. Huo, B. Gu, and H. Huang, "Training neural networks using features replay," *Advances in Neural Information Processing Systems*, vol. 31, 2018.
- [21] Z. Huo, B. Gu, H. Huang *et al.*, "Decoupled parallel backpropagation with convergence guarantee," in *International Conference on Machine Learning*. PMLR, 2018, pp. 2098–2106.
- [22] M. Jaderberg, W. M. Czarnecki, S. Osindero, O. Vinyals, A. Graves, D. Silver, and K. Kavukcuoglu, "Decoupled neural interfaces using synthetic gradients," in *International conference on machine learning*. PMLR, 2017, pp. 1627–1635.
- [23] A. Jain, A. A. Awan, A. M. Aljuhani, J. M. Hashmi, Q. G. Anthony, H. Subramoni, D. K. Panda, R. Machiraju, and A. Parwani, "Gems: Gpu-enabled memory-aware model-parallelism system for distributed dnn training," in *SC20: International Conference for High Performance Computing, Networking, Storage and Analysis*. IEEE, 2020, pp. 1–15.
- [24] Z. Jia, M. Zaharia, and A. Aiken, "Beyond data and model parallelism for deep neural networks," *Proceedings of Machine Learning and Systems*, vol. 1, pp. 1–13, 2019.
- [25] A. Krizhevsky, "One weird trick for parallelizing convolutional neural networks," *arXiv preprint arXiv:1404.5997*, 2014.
- [26] A. Krizhevsky, G. Hinton *et al.*, "Learning multiple layers of features from tiny images," 2009.
- [27] A. Krizhevsky, I. Sutskever, and G. E. Hinton, "Imagenet classification with deep convolutional neural networks," in *Proceedings of the 25th International Conference on Neural Information Processing Systems - Volume 1*, ser. NIPS'12. Red Hook, NY, USA: Curran Associates Inc., 2012, p. 1097–1105.
- [28] H. Kwon, A. Samajdar, and T. Krishna, "Maeri: Enabling flexible dataflow mapping over dnn accelerators via reconfigurable interconnects," *SIGPLAN Not.*, vol. 53, no. 2, p. 461–475, 2018. [Online]. Available: <https://doi.org/10.1145/3296957.3173176>
- [29] Y. A. LeCun, L. Bottou, G. B. Orr, and K.-R. Müller, *Efficient BackProp*. Berlin, Heidelberg: Springer Berlin Heidelberg, 2012, pp. 9–48. [Online]. Available: [https://doi.org/10.1007/978-3-642-35289-8\\_3](https://doi.org/10.1007/978-3-642-35289-8_3)
- [30] S. Li, T. Ben-Nun, S. D. Girolamo, D. Alistarh, and T. Hoefler, "Taming unbalanced training workloads in deep learning with partial collective operations," in *Proceedings of the 25th ACM SIGPLAN Symposium on Principles and Practice of Parallel Programming*, 2020, pp. 45–61.
- [31] S. Li and T. Hoefler, "Chimera: efficiently training large-scale neural networks with bidirectional pipelines," in *Proceedings of the International Conference for High Performance Computing, Networking, Storage and Analysis*, 2021, pp. 1–14.
- [32] T. P. Lillicrap, D. Cownden, D. B. Tweed, and C. J. Akerman, "Random synaptic feedback weights support error backpropagation for deep learning," *Nature communications*, vol. 7, no. 1, p. 13276, 2016.
- [33] T. Miyato, D. Okanohara, S.-i. Maeda, and M. Koyama, "Synthetic gradient methods with virtual forward-backward networks," 2017.
- [34] V. S. Naveen Muralimanohar, Ali Shafiee, "Cacti." [Online]. Available: <http://www.hpl.hp.com/research/cacti/>
- [35] A. Nøkland, "Direct feedback alignment provides learning in deep neural networks," *Advances in neural information processing systems*, vol. 29, 2016.
- [36] K. Papineni, S. Roukos, T. Ward, and W.-J. Zhu, "Bleu: a method for automatic evaluation of machine translation," in *Proceedings of the 40th annual meeting of the Association for Computational Linguistics*, 2002, pp. 311–318.
- [37] A. Paszke, S. Gross, F. Massa, A. Lerer, J. Bradbury, G. Chanan, T. Killeen, Z. Lin, N. Gimelshein, L. Antiga *et al.*, "Pytorch: An imperative style, high-performance deep learning library," *Advances in neural information processing systems*, vol. 32, 2019.
- [38] M. Peemen, A. A. Setio, B. Mesman, and H. Corporaal, "Memory-centric accelerator design for convolutional neural networks," in *2013 IEEE 31st International Conference on Computer Design (ICCD)*. IEEE, 2013, pp. 13–19.
- [39] T. Qiao, J. Zhang, D. Xu, and D. Tao, "Learn, imagine and create: Text-to-image generation from prior knowledge," in *Advances in Neural Information Processing Systems*, H. Wallach, H. Larochelle, A. Beygelzimer, F. d'Alché-Buc, E. Fox, and R. Garnett, Eds., vol. 32. Curran Associates, Inc., 2019. [Online]. Available: [https://proceedings.neurips.cc/paper\\_files/paper/2019/file/d18f655c3fce66ca401d5f38b48c89af-Paper.pdf](https://proceedings.neurips.cc/paper_files/paper/2019/file/d18f655c3fce66ca401d5f38b48c89af-Paper.pdf)

- [40] M. Sankaradas, V. Jakkula, S. Cadambi, S. Chakradhar, I. Durdanovic, E. Cosatto, and H. P. Graf, "A massively parallel coprocessor for convolutional neural networks," in *2009 20th IEEE International Conference on Application-specific Systems, Architectures and Processors*. IEEE, 2009, pp. 53–60.
- [41] A. Sergeev and M. Del Balso, "Horovod: fast and easy distributed deep learning in tensorflow," *arXiv preprint arXiv:1802.05799*, 2018.
- [42] D. Silver, T. Hubert, J. Schrittwieser, I. Antonoglou, M. Lai, A. Guez, M. Lanctot, L. Sifre, D. Kumaran, T. Graepel, T. Lillicrap, K. Simonyan, and D. Hassabis, "Mastering chess and shogi by self-play with a general reinforcement learning algorithm," 2017.
- [43] K. Simonyan and A. Zisserman, "Very deep convolutional networks for large-scale image recognition," *arXiv preprint arXiv:1409.1556*, 2014.
- [44] Synopsys, "Design compiler." [Online]. Available: <https://www.synopsys.com/implementation-and-signoff/rtl-synthesis-test/dc-ultra.html>
- [45] V. Sze, Y.-H. Chen, T.-J. Yang, and J. S. Emer, "Efficient processing of deep neural networks: A tutorial and survey," *Proceedings of the IEEE*, vol. 105, no. 12, pp. 2295–2329, 2017.
- [46] C. Szegedy, S. Ioffe, V. Vanhoucke, and A. Alemi, "Inception-v4, inception-resnet and the impact of residual connections on learning," 2016.
- [47] C. Szegedy, V. Vanhoucke, S. Ioffe, J. Shlens, and Z. Wojna, "Rethinking the inception architecture for computer vision," in *Proceedings of the IEEE conference on computer vision and pattern recognition*, 2016, pp. 2818–2826.
- [48] A. Vaswani, N. Shazeer, N. Parmar, J. Uszkoreit, L. Jones, A. N. Gomez, L. Kaiser, and I. Polosukhin, "Attention is all you need," 2017. [Online]. Available: <https://arxiv.org/abs/1706.03762>
- [49] A. Vaswani, N. Shazeer, N. Parmar, J. Uszkoreit, L. Jones, A. N. Gomez, L. Kaiser, and I. Polosukhin, "Attention is all you need," *Advances in neural information processing systems*, vol. 30, 2017.
- [50] Xilinx, "Virtex 7 fpga." [Online]. Available: <https://www.xilinx.com/products/silicon-devices/fpga/virtex-7.html>
- [51] Xilinx, "Vivado." [Online]. Available: <https://www.xilinx.com/products/design-tools/vivado.html>
- [52] D. Xu, A. Clappison, C. Seth, and J. Orchard, "Symmetric predictive estimator for biologically plausible neural learning," *IEEE Transactions on Neural Networks and Learning Systems*, vol. 29, no. 9, pp. 4140–4151, 2017.
- [53] Y. You, Z. Zhang, C.-J. Hsieh, J. Demmel, and K. Keutzer, "Imagenet training in minutes," in *Proceedings of the 47th International Conference on Parallel Processing*, 2018, pp. 1–10.
- [54] H. Zhuang, Y. Wang, Q. Liu, and Z. Lin, "Fully decoupled neural network learning using delayed gradients," *IEEE transactions on neural networks and learning systems*, vol. 33, no. 10, pp. 6013–6020, 2021.